

# Target mass corrections to parity-violating DIS

T. Hobbs

*Department of Physics and Center for Exploration of Energy and Matter,  
Indiana University, Bloomington, IN 47405, USA*

## Abstract

We examine the implications of several parameterizations of so-called target mass corrections (TMCs) for the physics of parity-violating deeply inelastic scattering (DIS), especially at high values of the momentum fraction  $x$ . We consider the role played by perturbative corrections in  $\alpha_S$  in modifying TMCs; we explicitly calculate these corrections at both the level of the individual electroweak structure function (SF), as well as in the observables of parity-violating DIS. TMCs augment an inventory of previously studied corrections that become sizable at low  $Q^2$  (finite- $Q^2$  corrections), and we give special attention to the effects that might lead to the violation of the approximate equality  $R^{\gamma Z} = R^\gamma$ .

PACS numbers: 25.30.Fj, 12.38.Bx, 13.60.Hb

Keywords: deeply inelastic scattering, target mass corrections, perturbative QCD

## I. INTRODUCTION

Recent developments in the drive to uncover the details of hadronic structure via high energy electron scattering have increased the interest in performing more precision measurements of nucleonic observables. Among such efforts is the push to extract partonic information at large values of the scaling variable Bjorken  $x$  [1]. Unfortunately, it is often at high  $x$  that various corrections that scale as  $1/Q^2$  or  $\log(Q^2)$  become significant and render measurements and their interpretation problematic. Typical of these kinds of corrections are target mass corrections (TMCs), which must be implemented as one moves away from the high-energy Bjorken limit at which the mass of the target nucleon may be neglected. The role of TMCs in electron-nucleon deeply inelastic scattering (DIS) at next-to-leading order (NLO) in  $\alpha_S$  is investigated here.

## II. TMC PRESCRIPTIONS

We calculate the TMCs in three main prescriptions: the conventional, leading-twist (LT) operator product expansion (OPE) of Georgi/Politzer,  $1/Q^2$  expansions of these LT corrections to various orders (which we take to be one formal prescription), and collinear factorization (CF). Historically well-established, the OPE has been thoroughly deployed in the careful analysis of TMCs to the (un)polarized structure functions (SFs) of DIS at leading perturbative order and at twist-2 and twist-3 [2]. In spite of this, there is a particular short-fall of the LT OPE treatment to provide the proper behavior of the mass-corrected SFs at kinematic threshold. This can be made evident by considering the corrected electroweak SFs as calculated in the LT OPE, and comparing these with the perturbative expansions of the same to  $O(1/Q^2)$  and  $O(1/Q^4)$ . As an example of one such SF that enters into the parity-violating asymmetry  $A^{PV}$ ,  $F_2^{\gamma Z}$  is calculated at NLO in  $\alpha_S$  at two scales:  $Q^2 = 2, 10$  GeV<sup>2</sup>. For simplicity, the left (right) column in all following plots corresponds to  $Q^2 = 2$  (10) GeV<sup>2</sup>. Here and in the following calculations, input SFs (that is, before the TMC is applied) are calculated according to standard quark-parton model (QPM) definitions with electroweak charges as given in the PDG. We notice that expansions to both orders of  $1/Q^2$  diverge from the LT calculation most at lowest  $Q^2$  and highest  $x$  as one might expect. This effect is illustrated in Figure 1.

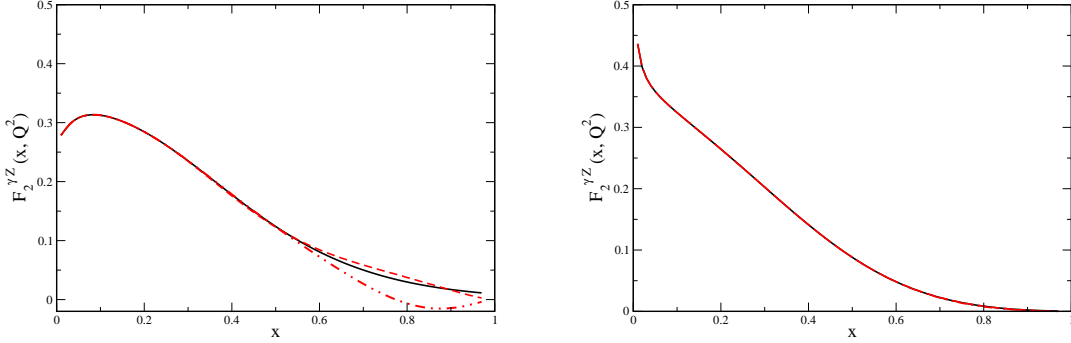


FIG. 1. We plot  $F_2^{\gamma Z}$  over the full kinematic range (i.e.,  $x \in [0, 1]$ ) for fixed  $Q^2$  following the implementation of the OPE (solid),  $O(1/Q^2)$  (dashed) and  $O(1/Q^4)$  (dot-dashed) corrections. The non-physical threshold behavior and negative down-turn are evident in the OPE and  $O(1/Q^4)$  curves, respectively.

To understand this behavior we recall that the corrected SFs in the Georgi/Politzer formalism are extracted via inverse Mellin transforms of the LT expansions of individual SF moments [3, 4] to obtain for spin-unpolarized DIS

$$\begin{aligned}
 F_1^{TMC}(x) &= \frac{x}{\xi\rho} F_1^{(0)}(\xi) + \frac{\mu x^2}{\rho^2} \int_{\xi}^1 du \frac{F_2^{(0)}(u)}{u^2} + \frac{2\mu^2 x^3}{\rho^3} \int_{\xi}^1 dv (v - \xi) \frac{F_2^{(0)}(v)}{v^2} \\
 F_2^{TMC}(x) &= \frac{x^2}{\xi^2 \rho^3} F_2^{(0)}(\xi) + \frac{6\mu x^3}{\rho^4} \int_{\xi}^1 du \frac{F_2^{(0)}(u)}{u^2} + \frac{12\mu^2 x^4}{\rho^5} \int_{\xi}^1 dv (v - \xi) \frac{F_2^{(0)}(v)}{v^2} \\
 F_3^{TMC}(x) &= \frac{x}{\xi\rho^2} F_3^{(0)}(\xi) + \frac{2\mu x^2}{\rho^3} \int_{\xi}^1 du \frac{F_3^{(0)}(u)}{u}, \quad (1)
 \end{aligned}$$

where  $\mu = M^2/Q^2$ , and  $\rho = \sqrt{1 + 4x^2 M^2/Q^2}$ ; we note also that the SFs appearing in Eqn (1) also contain some omitted dependence on  $Q^2$ . The LT results for  $F_2^{\gamma Z}$  are plotted as the solid curves of Figure 1. The associated dashed/dot-dashed curves are the  $O(1/Q^2)$  and  $O(1/Q^4)$  expansions of the LT result, respectively; we discuss the details of this calculation below.

A troubling ailment of the standard TMC treatment is evident in Figure 1: as one approaches the lowest accessible values of  $Q^2$ , the mass-corrected SFs attain zero only in the non-physical region  $x > 1$ ; that is, momentum conservation considerations would dictate that the electroweak SFs equal zero for  $x \geq 1$ . That this does not happen is an indication that the OPE incorporates some non-physical behavior in the move to low  $Q^2$ . One can understand

the origin of this non-physical behavior by recognizing that the standard GP prescription rescales the PDFs appearing in the QPM expressions for the SFs via the parameter

$$\xi(x, Q^2) = -\frac{q^+}{p^+} = \frac{2x}{1 + \rho}, \quad (2)$$

for which we note  $\xi(x, Q^2) \leq x$  for  $\mu \geq 0$ . As the SFs are monotonically decreasing functions of  $x$  for a given fixed  $Q^2$ , the rescaling forced by this procedure dictates that the corrected SFs are upward-shifted in magnitude, attaining zero only for  $\xi(x, Q^2) = 1$ . This occurs only for non-physical  $x \geq 1$ .

In the literature this issue has come to be referred to as the ‘threshold problem’ [5]. Several alternative prescriptions have been proposed to ameliorate this issue, including so-called collinear factorization, as well as a less formal approach that depends upon an  $O(1/Q^2)$  expansion of the LT OPE. The latter is motivated by the logic that it is the omission of the contributions from non-leading twist in the OPE that induces the threshold problem. Then, supposing that the  $O(1/Q^2)$  expansions simulate the higher twist contribution, one might anticipate that such an expansion would cure the non-physical behavior at large  $x$ . Again, a comparison of these perturbative expansions with the LT OPE are given in Figure 1 in the case of  $F_2^{\gamma Z}$ .

Via this treatment, we may expand Eqn (1) to LO in  $1/Q^2$  to obtain [6]

$$\begin{aligned} F_1^{TMC}(x, Q^2) &= (1 - \mu x^2)F_1^{(0)}(x) + \mu x^3 \cdot \left( \frac{2}{x} \int_x^1 \frac{dz}{z^2} F_1^{(0)}(z) - \frac{\partial}{\partial x} F_1^{(0)}(x) \right) \\ F_2^{TMC}(x, Q^2) &= (1 - 4\mu x^2)F_2^{(0)}(x) + \mu x^3 \cdot \left( 6 \int_x^1 \frac{dz}{z^2} F_2^{(0)}(z) - \frac{\partial}{\partial x} F_2^{(0)}(x) \right) \\ F_3^{TMC}(x, Q^2) &= (1 - 3\mu x^2)F_3^{(0)}(x) + \mu x^3 \cdot \left( \frac{2}{x} \int_x^1 \frac{dz}{z^2} F_3^{(0)}(z) - \frac{\partial}{\partial x} F_3^{(0)}(x) \right), \end{aligned} \quad (3)$$

where there is again an understood  $Q^2$  dependence for all SFs on the right. The result of calculating  $F_2^{\gamma Z}$  as given in Eqn (3) over a range of  $x$  for low and intermediate  $Q^2$  is given as the dashed curves in Figure 1. While there has been interest expressed in the literature for attempting to solve the non-physical behavior at kinematic threshold with such an expansion, this procedure has only previously been carried out to  $O(1/Q^2)$ . It is therefore sensible to carry out the expansion to an additional perturbative order in  $1/Q^2$  to gauge if this provides further improvement in forcing the corrected SFs to observe the limit

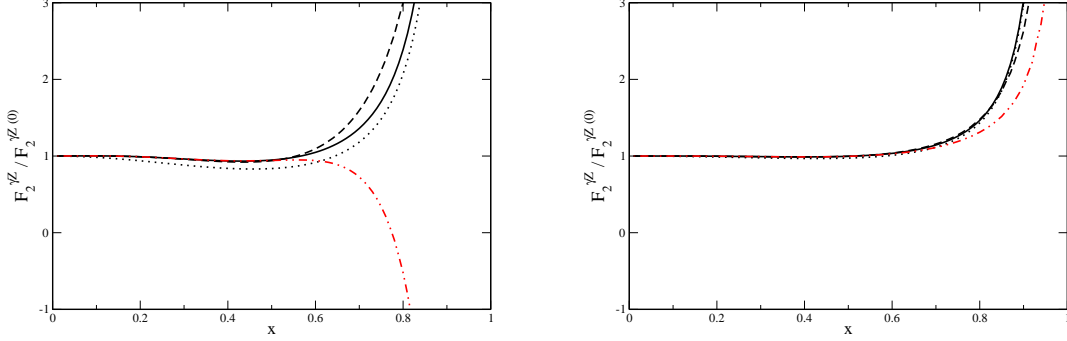


FIG. 2. When plotted as a ratio  $F^{TM C}/F^{(0)}$ , the negative downturn at low  $Q^2$  obtained in the  $O(1/Q^4)$  (dot-dashed) expansion is more evident. We compare this to the OPE (solid),  $O(1/Q^2)$  (dashed), and CF (dotted) prescriptions.

$F_i^{TM C}(x=1, Q^2) = 0$ . Expanding the expressions in Eqn (1) still further, we get

$$\begin{aligned}
 F_1^{O(1/Q^4)}(x, Q^2) = \dots \mu^2(2x^3 g_2(x, Q^2) - 4x^4 h_2(x, Q^2) + x^3 F_2^{(0)}(x, Q^2) \\
 + 3x^4 F_1^{(0)}(x, Q^2) + 3x^5 F_1^{\prime(0)}(x, Q^2) + \frac{x^6}{2} F_1^{\prime\prime(0)}(x, Q^2))
 \end{aligned} \tag{4}$$

$$\begin{aligned}
 F_2^{O(1/Q^4)}(x, Q^2) = \dots \mu^2(12x^4 g_2(x, Q^2) - 48x^5 h_2(x, Q^2) + 23x^4 F_2^{(0)}(x, Q^2) \\
 + 6x^5 F_2^{\prime(0)}(x, Q^2) + \frac{x^6}{2} F_2^{\prime\prime(0)}(x, Q^2))
 \end{aligned} \tag{5}$$

$$\begin{aligned}
 F_3^{O(1/Q^4)}(x, Q^2) = \dots \mu^2(-12x^4 h_3(x, Q^2) + 13x^4 F_3^{(0)}(x, Q^2) + 5x^5 F_3^{\prime(0)}(x, Q^2) \\
 + \frac{x^6}{2} F_3^{\prime\prime(0)}(x, Q^2)).
 \end{aligned} \tag{6}$$

The dot-dashed curves of Figure 1 are obtained then from plotting  $F_2^{\gamma Z}$  from Eqn (5) similarly to the GP and  $O(1/Q^2)$  curves. Notable here is the fact that while the  $O(1/Q^4)$  expansion predictably forces the corrected SFs more strongly to observe the zero limit at the kinematic threshold, it introduces a separate, non-physical behavior distinct from the threshold problem. This becomes obvious at lowest  $Q^2$  and highest  $x$  and is thus an artifact of the regime in which the expansion parameter  $1/Q^2$  becomes large. In Figure 1, the corrected SF becomes negative for  $x \geq 0.8$ . We illustrate this effect more explicitly in Figure 2, in which we plot a ratio of corrected to uncorrected SFs. As the cross section is expressed in terms of these electroweak SFs, and is by the optical theorem a non-negative physical

observable, we demand that the SFs be positive-definite as well. By this logic, the negative downturn evident in Figures 1, 2, etc., is prohibited. That the higher order terms of the  $1/Q^2$  expansion induce this non-physical behavior calls into question the unlimited validity of such an approach – at least when extended to too low  $Q^2$ .

For completeness, we calculate effects in physical observables using the previously mentioned CF approach also. This method relies upon a choice of frame such that (in DIS) the virtual photon and nucleon light-cone momenta are collinear; the resulting cross section and SFs may then be expressed as a convolution of a perturbatively calculable hard coefficient with the universal PDFs in a fashion that directly incorporates the nucleon mass [7, 8]:

$$F_i(x, Q^2) = \sum_f \int_{x_{min}}^{x_{max}} \frac{dx}{x} h_i^f(x_f, Q^2) \phi_{f/N}(x, Q^2). \quad (7)$$

Here the bounds of integration  $x_{min}, x_{max}$  are fixed by the mass-dependent kinematics. In the case of the SF  $F_2$ , this procedure yields a correction of the form

$$F_2(x, Q^2) = \frac{x}{x_f} \frac{\rho_f^2}{\rho^2} h_2^f \otimes \phi_{f/N}(\xi), \quad (8)$$

in which  $x_f, \rho_f$  are partonic analogs of Bjorken  $x$  and the previously defined  $\rho$  parameter.

### III. TMCS IN THE OBSERVABLES OF DIS

Ultimately, we wish to obtain a prescription-independent estimate of the magnitude of the effect of TMCs in measurements of typical DIS observables, such as the parity-violating asymmetry particular to electron-proton scattering. As far as experimental efforts to determine the high- $x$  structure of the nucleon are concerned, there is no *a priori* knowledge of the size of the possible contribution from TMCs, and a thorough theoretical analysis is needed to ensure that the extraction of desired signals (such as the density function ratio  $d/u$ ) is not imperiled.

As noted, there is considerable experimental interest in more precise determinations of the sensitivity of the parity-violating asymmetry  $A^{PV}$  to the flavor structure of the nucleon. For electromagnetic and interference currents, the asymmetry may be expressed as [9]

$$A^{PV} = - \left( \frac{G_F Q^2}{4\sqrt{2}\pi\alpha} \right) \left[ g_A^e Y_1 \frac{F_1^{\gamma Z}}{F_1^\gamma} + \frac{g_V^e}{2} Y_3 \frac{F_3^{\gamma Z}}{F_1^\gamma} \right], \quad (9)$$

in which the parameters  $Y_1, Y_3$  are given by

$$Y_1 = \frac{1 + (1 - y)^2 - y^2(1 - r^2/(1 + R^{\gamma Z})) - 2xyM/E}{1 + (1 - y)^2 - y^2(1 - r^2/(1 + R^\gamma)) - 2xyM/E} \left( \frac{1 + R^{\gamma Z}}{1 + R^\gamma} \right),$$

$$Y_3 = \frac{1 - (1 - y)^2}{1 + (1 - y)^2 - y^2(1 - r^2/(1 + R^\gamma)) - 2xyM/E} \left( \frac{r^2}{1 + R^\gamma} \right). \quad (10)$$

In particular we note that  $Y_1, Y_3$  depend upon the ratios of longitudinal/transverse virtual photon cross sections,

$$R^{\gamma(\gamma Z)} \equiv \frac{\sigma_L^{\gamma(\gamma Z)}}{\sigma_T^{\gamma(\gamma Z)}} = r^2 \frac{F_2^{\gamma(\gamma Z)}}{2xF_1^{\gamma(\gamma Z)}} - 1. \quad (11)$$

Consequently, to understand the mass effect in the full asymmetry, it is important first to grasp TMCs in the setting of the electroweak  $R$  parameters.

There is a standing corpus of phenomenology [10, 11] to describe the electromagnetic ratio  $R^\gamma$ , but the corresponding interference quantity  $R^{\gamma Z}$  is largely undetermined. In the interest of controlling uncertainties induced by  $R^{\gamma Z} \neq R^\gamma$ , an understanding of the physics that might differently break the partonic Callan-Gross relations for purely electromagnetic and interference processes is needed. Insofar as Callan-Gross is strictly observed by the parton model at LO, we expect  $R^{\gamma Z} = R^\gamma$  to be broken by perturbative corrections in  $\alpha_S$ , possible contributions from beyond twist-4, TMCs, and other non-perturbative physics. In an effort to understand the role of NLO corrections and TMCs in producing  $R^{\gamma Z} \neq R^\gamma$ , we plot a ratio of the interference to electromagnetic  $R$  parameters in the presence of mass corrections and at NLO. We compute this ratio using the definitions of Eqn (11), in which the parton model expressions for the SFs are typical of proton (Figure 3) and deuteron (Figure 4) scattering. The results, which are largely independent of  $Q^2$ , establish the largest deviation from  $R^{\gamma Z}/R^\gamma = 1$  at low  $x$ , where the effect has a magnitude  $\approx 5\%$ . This becomes more shallow as one moves to highest  $x$ ; also of note is the fact that TMCs undermine the correction to  $R^{\gamma Z}/R^\gamma$  due to calculation at NLO.

The picture of the breaking of  $R^{\gamma Z} = R^\gamma$  is qualitatively similar for the deuteron, but with the size of the effect diminished by several percent. As with the proton calculation, the strongest departure of the ratio plotted in Figure 4 from unity is obtained at low  $x$  – in this case  $x \approx 0.05 - 0.1$ , at which  $R^{\gamma Z}/R^\gamma \approx 0.985$ . This smaller effect is consistent with the nature of the deuteron as an iso-scalar target, which leads to the large-scale cancellation of flavor-dependence.

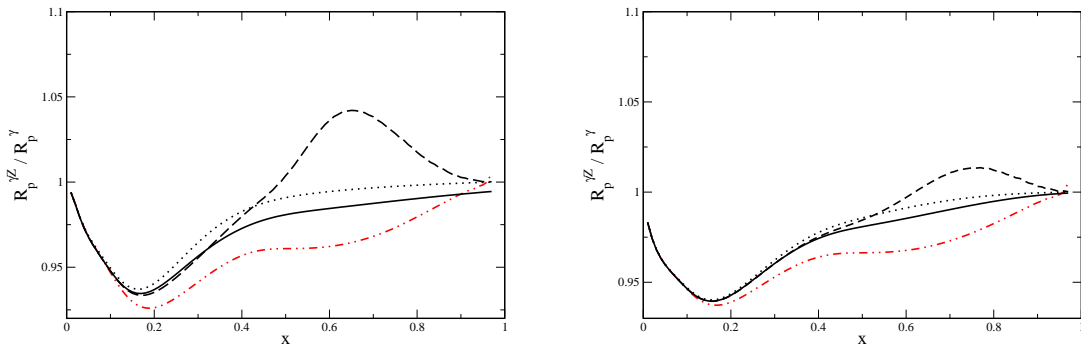


FIG. 3. An illustration of the breaking of the  $R^{\gamma Z} = R^\gamma$  induced by the target mass and perturbative corrections. We plot a ratio  $R^{\gamma Z}/R^\gamma$  as obtained in proton scattering. The dot-dashed curve is generated in the absence of TMCs but at NLO, whereas the solid (OPE), dashed ( $1/Q^2$  expansion), and dotted (CF) curves include the nucleon mass effect as well.

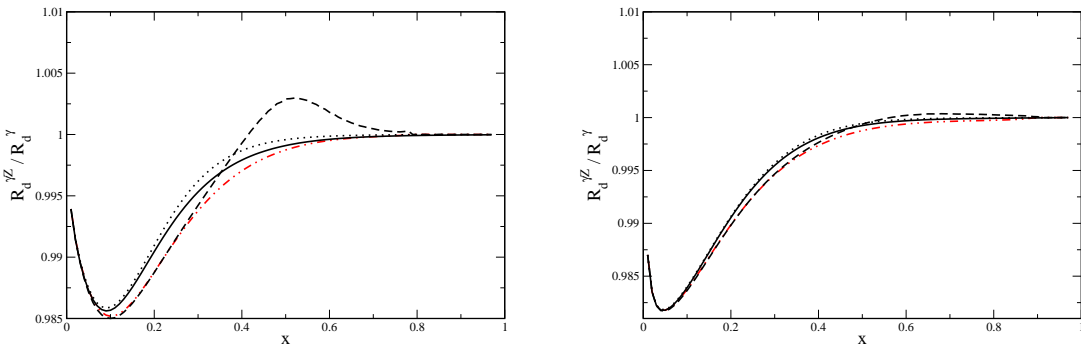


FIG. 4. Similar to Figure 3, but for  $R^{\gamma Z}/R^\gamma$  as determined in electron-deuteron scattering. Here, the nature of the deuteron as an iso-scalar target softens the breaking of  $R^{\gamma Z} = R^\gamma$ . The conventions for the linestyles are identical to Figure 3.

With some understanding of the behavior of  $R^{\gamma Z}$  and  $R^\gamma$  under TMCs, we wish to perform a similar calculation in the full, parity-violating asymmetry  $A^{PV}$ . As before, we consider a ratio of corrected/uncorrected asymmetries in the various prescriptions; the result of this calculation at low and intermediate  $Q^2$  is given in Figure 5. For low  $Q^2$ , we note a relative similarity among the various prescriptions to intermediate  $x \approx 0.6$  at which the effect of TMCs is  $\approx 6\%$ ; as one moves to largest  $x$ , the OPE and CF treatments obtain the greatest effect ( $\approx 8\%$ ), whereas the  $O(1/Q^2)$  expansion of the LT OPE falls to zero. These effects



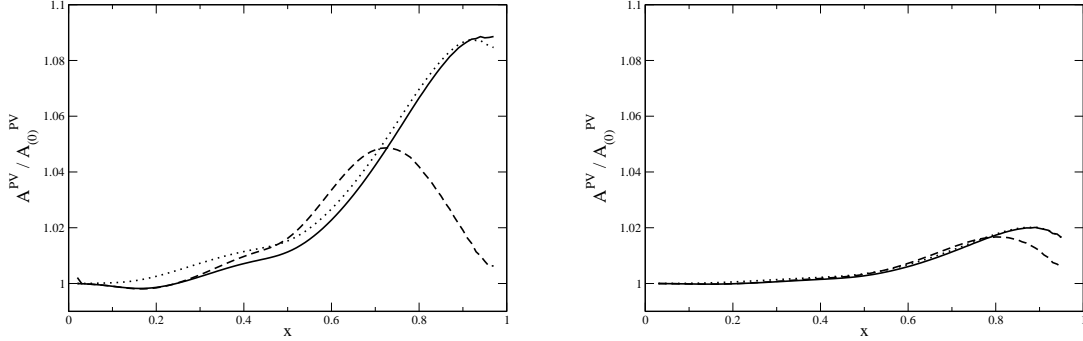


FIG. 5. The mass effect in the parity-violating asymmetry  $A^{TMC}/A^{(0)}$  at low and intermediate  $Q^2$ . We plot the mass effect in our three primary prescriptions – the OPE (solid),  $O(1/Q^2)$  expansion (dashed), and CF (dotted) treatments.

are quickly suppressed as one evolves to intermediate  $Q^2 = 10 \text{ GeV}^2$  for which the TMCs are  $\leq 2\%$ , and the  $O(1/Q^2)$  expansion agrees with the other prescriptions to higher  $x$ . This observation is consistent with the general message for experimental efforts: though mass effects can be sizable for lower values of  $Q^2$ , they may be brought into considerable control by moving to modestly larger  $Q^2$  at which the computed TMCs exhibit less model-dependence.

It is natural to extend this calculation to the deuteron, for which the property of isoscalarity diminishes flavor-dependence as previously noted; the resulting asymmetry is dependent only on the electroweak couplings and the kinematical parameters  $Y_1, Y_3$  [9]:

$$A^{\text{PV}} = - \left( \frac{3G_F Q^2}{10\sqrt{2}\pi\alpha} \right) [Y_1 (2C_{1u} - C_{1d}) + Y_3 (2C_{2u} - C_{2d})] , \quad (12)$$

where the  $C_{1u}, C_{1d}$ , etc are coupling constants. The disappearance of the explicit dependence of the deuteron asymmetry on SFs leads to a very small sensitivity to TMCs: generally, even at small  $Q^2$ , the mass effect in the deuteron is sub-percent and model-independent in the sense that the various prescriptions outlined here yield similarly small corrections. This is promising for experimental efforts that aim (for instance) to precisely extract the electroweak coupling constants from electron-deuteron scattering events.

Lastly, as the SF ratio  $R_{n/p} = F_2^n/F_2^p$  is sensitive to the behavior of the PDF ratio  $d/u$ , it has attracted substantial interest as a means of constraining various quark models. This is apparent if we observe, for example, that if the large- $x$  ratio  $d/u \rightarrow 0$ , then the SF ratio behaves as  $R_{n/p} \rightarrow -\frac{1}{2}C_{1d}/C_{1u} \approx 0.9$ . Given this interest in the phenomenology of  $R^{n/p}$

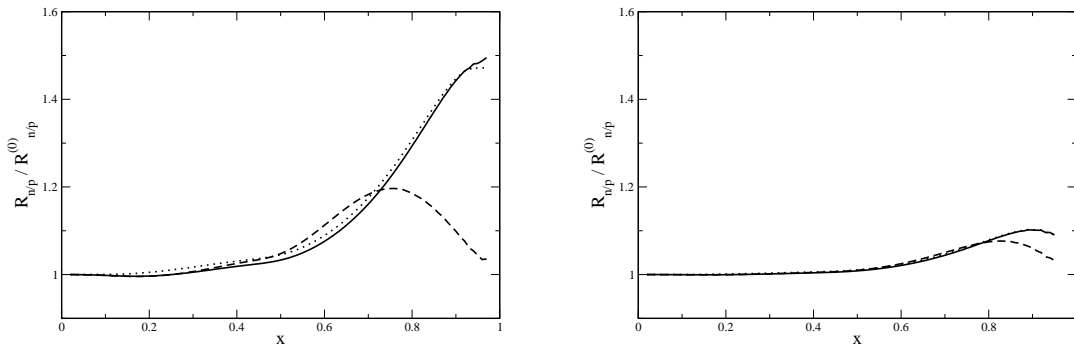


FIG. 6. The TMC effect in the SF ratio  $R_{n/p} = F_2^n/F_2^p$ . As with Figure 5, the prescriptions are the OPE (solid),  $O(1/Q^2)$  expansion (dashed), and CF (dotted).

(particularly at large  $x$  where TMCs are often more pronounced), a picture of the mass corrections to  $R^{n/p}$  would be helpful. Such an illustration of the relative mass effect is given in Figure 6. As with  $A^{PV}$  we plot a correction ratio  $R_{n/p}/R_{n/p}^{(0)}$  for  $Q^2 = 2(10)$   $\text{GeV}^2$ , and obtain a result which qualitatively closely resembles the full proton asymmetry – up to the scale of the effect. Here again, the size of the correction, as well as the agreement among the various prescriptions are dramatically improved by modestly evolving upward in  $Q^2$ .

In conclusion, while the TMCs and perturbative corrections in  $\alpha_S$  are considerable at lowest  $Q^2$  where other  $1/Q^2$  and  $\log(Q^2)$  effects become important, they may be controlled in experimental efforts. In particular, performing measurements at higher  $Q^2$  and choosing iso-scalar targets enables one to cleanly probe nucleon structure with less need to worry about possible model-dependent mass effects. Still, the issues of the kinds of physics that might produce  $R^{\gamma Z} \neq R^\gamma$  and the possible implications for high- $x$  phenomenology remain rich and largely unexplored topics.

## ACKNOWLEDGMENTS

We thank W. Melnitchouk, A. Accardi, J. Owens, M. Ramsey-Musolf, K. Kumar, and P. Souder for valuable discussions and communications.

---

[1] P. A. Souder, AIP Conf. Proc. **747**, 199-204 (2005).

- [2] J. Blumlein and A. Tkabladze, Nucl. Phys. B **553** (1999) 427 [arXiv:hep-ph/9812478].
- [3] H. Georgi, H. D. Politzer, Phys. Rev. **D14**, 1829 (1976).
- [4] O. Nachtmann, Nucl. Phys. **B63**, 237-247 (1973).
- [5] I. Schienbein, V. A. Radescu, G. P. Zeller *et al.*, J. Phys. G **G35**, 053101 (2008). [arXiv:0709.1775 [hep-ph]].
- [6] S. A. Kulagin, R. Petti, Nucl. Phys. **A765**, 126-187 (2006). [hep-ph/0412425].
- [7] A. Accardi, J. -W. Qiu, JHEP **0807**, 090 (2008). [arXiv:0805.1496 [hep-ph]].
- [8] A. Accardi, T. Hobbs, W. Melnitchouk, JHEP **0911**, 084 (2009). [arXiv:0907.2395 [hep-ph]].
- [9] T. Hobbs, W. Melnitchouk, Phys. Rev. **D77**, 114023 (2008). [arXiv:0801.4791 [hep-ph]].
- [10] S. A. Kulagin, R. Petti, Phys. Rev. **D76**, 094023 (2007). [hep-ph/0703033 [HEP-PH]].
- [11] L. W. Whitlow, S. Rock, A. Bodek *et al.*, Phys. Lett. **B250**, 193-198 (1990).